Similarity theory and calculation of turbulent fluxes at the surface for the stably stratified atmospheric boundary layer

Sergej S. Zilitinkevich · Igor N. Esau

Abstract In this paper we revise the similarity theory for the stably stratified atmospheric boundary layer (ABL), formulate analytical approximations for the wind velocity and potential temperature profiles over the entire ABL, validate them against large-eddy simulation and observational data, and develop an improved surface flux calculation technique for use in operational models.

Keywords Monin–Obukhov similarity theory · Planetary boundary layer · Prandtl number · Richardson number · Stable stratification · Surface fluxes in atmospheric models · Surface layer

1 Introduction

Parameterisation of turbulence in atmospheric models comprises two basic problems:

- turbulence closure—to calculate vertical turbulent fluxes, first of all, the fluxes of momentum and potential temperature: $\vec{\tau}$ and F_θ through the mean gradients: $d\vec{U}/dz$ and $d\Theta/dz$ (where z is the height, $\vec{U}$ and Θ are the mean wind speed and potential temperature);
- flux–profile relationships—to calculate the fluxes at the earth's surface: $\tau_* = \tau|_{z=0}$ and $F_* = F_\theta|_{z=0}$ through the mean wind speed $U_1 = U|_{z=z_1}$ and potential temperature $\Theta_1 = \Theta|_{z=z_1}$ at a given level, z_1, above the surface.

S. S. Zilitinkevich (✉)
Division of Atmospheric Sciences, University of Helsinki, Helsinki, Finland
e-mail: sergej.zilitinkevich@fmi.fi

I. N. Esau · S. S. Zilitinkevich
Nansen Environmental and Remote Sensing Centre/Bjerknes Centre for Climate Research, Bergen, Norway

S. S. Zilitinkevich
Finnish Meteorological Institute, Helsinki, Finland

doi: 10.1007/978-0-387-74321-9_4,

We focus on the flux–profile relationships for stable and neutral stratifications. At first sight, these could be obtained numerically using an adequate turbulence-closure model. However, this way is too computationally expensive: the mean gradients close to the surface are very sharp, which requires very high resolution, not to mention that the adequate closure for strongly stable stratification can hardly be considered as a fully understood, easy problem. Hence the practically sound problem is to analytically express the surface fluxes τ_* and F_* through $U_1 = U|_{z=z_1}$ and $\Theta_1 = \Theta|_{z=z_1}$ available in numerical models (and similarly for the fluxes of humidity and other scalars). In numerical weather prediction (NWP) and climate models, the lowest computational level is usually taken $z_1 \approx 30\,\text{m}$ (see Ayotte et al. 1996; Tjernstrom 2004).

In neutral or near-neutral stratification the solution to the above problem is given by the logarithmic wall law:

$$\frac{dU}{dz} = \frac{\tau^{1/2}}{kz}, \tag{1a}$$

$$\frac{d\Theta}{dz} = \frac{-F_\theta}{k_T \tau^{1/2} z}, \tag{1b}$$

$$U = \frac{\tau^{1/2}}{k} \ln \frac{z}{z_{0u}}, \tag{1c}$$

$$\Theta = \Theta_s + \frac{-F_\theta}{k_T \tau^{1/2}} \ln \frac{z}{z_{0T}}, \tag{1d}$$

$$\Theta_0 + \frac{-F_\theta}{k_T \tau^{1/2}} \ln \frac{z}{z_{0u}}, \tag{1e}$$

where k and k_T are the von Karman constants, z_{0u} and z_{0T} are the roughness lengths for momentum and heat, Θ_s is the potential temperature at the surface, and Θ_0 is the aerodynamic surface potential temperature, that is the value of $\Theta(z)$ extrapolated logarithmically down to the level $z = z_{0u}$ [determination of the difference $\Theta_0 - \Theta_s = k_T^{-1}(-F_\theta \tau^{-1/2}) \ln(z_{0u}/z_{0T})$ comprises an independent problem; see, e.g., Zilitinkevich et al. (2001, 2002)]. As follows from Eq. 1, $\tau_1^{1/2} = kU_1(\ln z/z_{0u})^{-1}$ and $F_{\theta 1} = -kk_T U_1(\Theta_1 - \Theta_0)(\ln z/z_{0u})^{-2}$. The turbulent fluxes τ_1 and $F_{\theta 1}$ at the level $z = z_1$ can be identified with the surface fluxes: $\tau_1 = \tau_*$ and $F_{\theta 1} = F_*$, provided that z_1 is much less then the height, h, of the atmospheric boundary layer (ABL). In neutral stratification, a typical value of h is a few hundred metres, so that the requirement $z_1 \approx 30\,\text{m} \ll h$ is satisfied.

In stable stratification, the problem becomes more complicated. Its commonly accepted solution is based, firstly, on the assumption that the level z_1 belongs to the surface layer [that is the lowest one tenth of the ABL, where the turbulent fluxes do not diverge considerably from their surface values: $\tau \approx \tau_*$ and $F_\theta \approx F_*$] and, secondly, on the Monin–Obukhov (MO) similarity theory for surface-layer turbulence (Monin and Obukhov 1954).

The MO theory states that the turbulent regime in the stratified surface layer is fully characterised by the turbulent fluxes, $\tau \approx \tau_* = u_*^2$ (where u_* is the friction velocity) and $F_\theta \approx F_*$, and the buoyancy parameter, $\beta = g/T_0$ (where g is the acceleration of gravity, and T_0 is a reference value of absolute temperature), which determine the familiar Obukhov length scale

$$L = \frac{\tau^{3/2}}{-\beta F_\theta}, \tag{2}$$

whereas the velocity and potential temperature gradients are expressed through universal functions, Φ_M and Φ_H, of the dimensionless height $\xi = z/L$:

$$\frac{kz}{\tau^{1/2}}\frac{dU}{dz} = \Phi_M(\xi), \tag{3a}$$

$$\frac{k_T\tau^{1/2}z}{-F_\theta}\frac{d\Theta}{dz} = \Phi_H(\xi). \tag{3b}$$

From the requirement of consistency with the wall law for neutral stratification, Eq. 1, it follows that $\Phi_M = \Phi_H \to 1$ at $\xi \ll 1$. The asymptotic behaviour of Φ_M and Φ_H in strongly stable stratification (at $\xi \gg 1$) is traditionally derived from the concept of z-less stratification, which states that at $z \gg L$ the distance above the surface, z, no longer affects turbulence. If so, the velocity- and temperature-gradient formulations should become independent of z, which immediately suggests the linear asymptotes: $\Phi_M \sim \Phi_H \sim \xi$. The linear interpolation between the neutral and the strong stability limits gives

$$\Phi_M = 1 + C_{U1}\xi, \tag{4a}$$

$$\Phi_H = 1 + C_{\Theta1}\xi, \tag{4b}$$

where C_{U1} and $C_{\Theta1}$ are empirical dimensionless constants.

The above analysis is usually considered as relevant only to the surface layer. However, the basic statement of the MO similarity theory, namely, that surface-layer turbulence is fully characterised by τ, F_θ and β, is applicable to locally generated turbulence in a more general context. Nieuwstadt (1984) was probably the first who extended the MO theory by substituting the height-dependent τ and F_θ for the height-constant τ_* and F_*, and demonstrated its successful application to the entire nocturnal stable ABL. In the present paper we employ this extended version of the MO theory.

In the surface layer, substituting Eq. 4 for Φ_M and Φ_H into Eq. 3 and integrating over z, yields the log-linear approximation:

$$U = \frac{u_*}{k}\left(\ln\frac{z}{z_{u0}} + C_{U1}\frac{z}{L_s}\right), \tag{5a}$$

$$\Theta - \Theta_0 = \frac{-F_*}{k_T u_*}\left(\ln\frac{z}{z_{u0}} + C_{\Theta1}\frac{z}{L_s}\right), \tag{5b}$$

where $L_s = u_*^3(-\beta F_*)^{-1}$.

Since the late 1950s, Eqs. 3–5 have been compared with experimental data in numerous works that basically gave estimates of C_{U1} close to 2 and $C_{\Theta1}$ also close to 2 but with a wider spread (see overview by Högström 1996; Yague et al., 2006). Experimentalists often admitted that for Θ the log-linear formulation is worse than for U (e.g., the above reference) but no commonly accepted alternative formulations were derived from physical grounds. Esau and Byrkjedal (2007) analysed data from large-eddy simulations (LES) and disclosed that the coefficient $C_{\Theta1}$ in Eq. 4b is not a constant but increases with increasing z/L.

According to Eqs. 3–4 the Richardson number, Ri$\equiv \beta(d\Theta/dz)(dU/dz)^{-2}$, monotonically increases with increasing z/L, and at $z/L \to \infty$ achieves its maximum value: $\mathrm{Ri}_c = k^2C_{\Theta1}k_T^{-1}C_{U1}^{-2}$. In other words, Eq. 4 is not applicable to Ri $>$ Ri$_c$. This conclusion is consistent with the critical Richardson number concept, universally accepted at the time when the MO theory and Eqs. 3–5 were formulated.

However, as recognised recently, the concept of the critical Ri contradicts both experimental evidence and analysis of the turbulent kinetic and potential energy budgets (see Zilitinkevich et al. 2007b). This conclusion is by no means new. Long ago it has been understood that turbulent closures or surface flux schemes implying the critical Ri lead to erroneous conclusions, such as unrealistic decoupling of air flows from the underlying surface in all cases when Ri> Ri_c. It is not surprising that modellers do not use Eq. 4 as well as other formulations of similar type, even though they are supported by experimental data. Instead, operational modellers develop their own flux–profile relationships, free of the critical Ri, and evaluate them indirectly—fitting the model results to the available observational data. Different points of view of experimentalists and operational modellers on the flux–profile relationships have factually caused two nearly independent lines of inquiry in this field (see discussion in Zilitinkevich et al. 2002).

One more point deserves emphasising. Currently used flux-calculation schemes identify the turbulent fluxes calculated at the level z_1 with the surface fluxes. However, in strongly stable stratification, especially in the long-lived stable ABL, the ABL height, h, quite often reduces to a few dozen metres[1] (see Zilitinkevich and Esau 2002, 2003; Zilitinkevich et al. 2007a) and becomes comparable with z_1 adopted in operational models. In such cases τ_1 and $F_{\theta 1}$ have nothing in common with τ_* and F_*.

Furthermore, the MO theory, considered for half a century as an ultimate framework for analysing the surface-layer turbulence, is now revised. Zilitinkevich and Esau (2005) have found that, besides L, Eq. 2, which characterise the stabilising effect of local buoyancy forces on turbulence, there are two additional length scales: L_f characterising the effect of the Earth's rotation and L_N characterizing the non-local effect of the static stability in the free atmosphere above the ABL:

$$L_N = \frac{\tau^{1/2}}{N}, \tag{6a}$$

$$L_f = \frac{\tau^{1/2}}{|f|}, \tag{6b}$$

where f is the Coriolis parameter, and $N = (\beta \partial \Theta / \partial z)^{1/2}$ is the Brunt-Väisälä frequency above the ABL. For certainty, we determine N from the temperature profile in the height interval $h < z < 2h$ (see Zilitinkevich and Esau 2005). Its typical atmospheric value is $N \sim 10^{-2}\,\mathrm{s}^{-1}$. Interpolating between the squared reciprocals of the three scales (which gives larger weights to stronger mechanisms that is to smaller scales) a composite turbulent length scale becomes:

$$\frac{1}{L_*} = \left[\left(\frac{1}{L}\right)^2 + \left(\frac{C_N}{L_N}\right)^2 + \left(\frac{C_f}{L_f}\right)^2\right]^{1/2}, \tag{7}$$

where $C_N = 0.1$ and $C_f = 1$ are empirical dimensionless coefficients.[2] Advantages of this scaling have been demonstrated in the plots of Φ_M and Φ_H versus z/L_* (Figs. 2 and 5 in *op. cit.*) showing an essential collapse of data points compared to the traditional plots of Φ_M and Φ_H vs. z/L.

1 The ABL height is defined as the level at which the turbulent fluxes become an order of magnitude smaller than close to the surface.

2 In *op. cit.* the coefficient C_N was taken 0.1 for Φ_M and 0.15 for Φ_H. Further analysis has shown that the difference is insignificant, which allows employing one composite length scale given by Eq. 7.

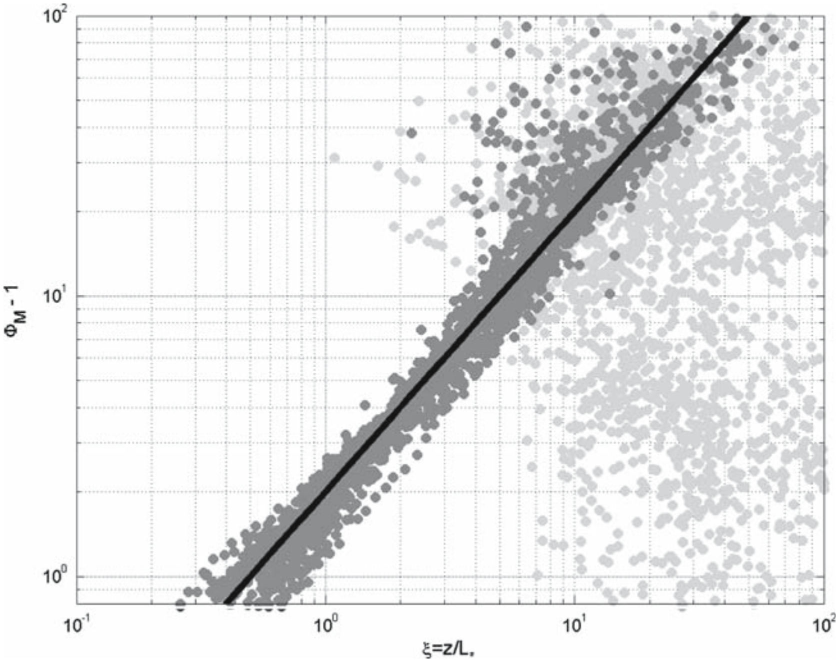

Fig. 1 Dimensionless velocity gradient, $\Phi_M = \frac{kz}{\tau^{1/2}}\frac{dU}{dz}$, in the ABL ($z < h$) and above ($z > h$) versus dimensionless height $\xi = z/L_*$, after the LES DATABASE64. Dark grey points show data for $z < h$; light grey points, for $z > h$; the line shows Eq. 11a with $C_{U1} = 2$

Practical application of this scaling requires information about vertical profiles of turbulent fluxes across the ABL. As demonstrated by Lenshow et al. (1988), Sorbjan (1988), Wittich (1991), Zilitinkevich and Esau (2005) and Esau and Byrkjedal (2007), the ratios τ/τ_* and F_θ/F_* are reasonably accurately approximated by universal functions of z/h, where h is the ABL height (see Eq. 15 below).

As follows from the above discussion, currently used surface-flux calculation schemes need to be improved accounting for

- modern experimental evidence and theoretical developments arguing against the critical Ri concept,
- additional mechanisms and scales, first of all L_N, disregarded in the classical similarity theory for the stable ABL,
- essential difference between the surface fluxes and the fluxes at $z = z_1$.

In the present paper we attempt to develop a new scheme applicable to as wide as possible a range of stable and neutral ABL regimes using recent theoretical developments and new, high quality observations and LES.

2 Mean gradients and the Richardson number

Until recently the ABL was distinguished accounting for only one factor, the potential temperature flux at the surface, F_*: neutral ABL at $F_* = 0$, and stable ABL at $F_* < 0$. Accounting

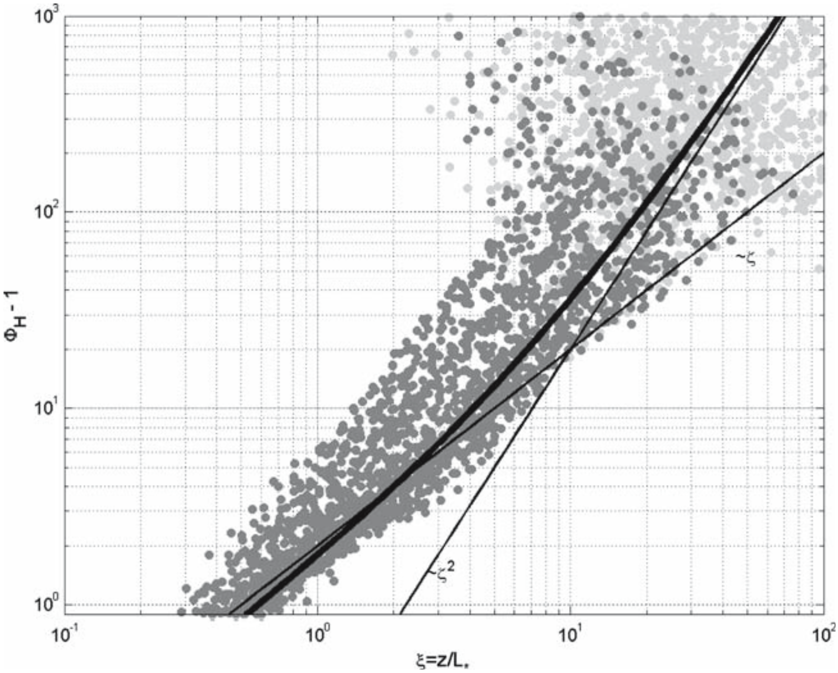

Fig. 2 Same as in Fig. 1 but for the dimensionless potential temperature gradient, $\Phi_H = \frac{k_T \tau^{1/2} z}{-F_\theta} \frac{d\Theta}{dz}$. The bold curve shows Eq. 11b with $C_{\Theta 1} = 1.6$ and $C_{\Theta 2} = 0.2$; the thin lines show its asymptote $\Phi_H = 0.2\xi^2$ and the traditional approximation $\Phi_H = 1 + 2\xi$

for the recently disclosed role of the static stability above the ABL, we now apply a more detailed classification:

- truly neutral (TN) ABL: $F_* = 0$, $N = 0$,
- conventionally neutral (CN) ABL: $F_* = 0$, $N > 0$,
- nocturnal stable (NS) ABL: $F_* < 0$, $N = 0$,
- long-lived stable (LS) ABL: $F_* < 0$, $N > 0$.

Realistic surface-flux calculation schemes should be based on a model applicable to all these types of ABL.

As mentioned in Sect. 1, Eq. 4b gives erroneous asymptotic behaviour at large $\xi = z/L$ and leads to the appearance of the critical Ri. This conclusion is sometimes treated as a failure of the MO theory, but this is not the case. The MO theory states only that Φ_M and Φ_H are universal functions of ξ, whereas the linear forms of the Φ functions, Eq. 4, are derived form the heuristic concept of z-less stratification, which is neither proved theoretically nor confirmed by experimental data.

In fact, this concept is not needed to derive the linear asymptotic formula for the velocity gradient in stationary, homogeneous, sheared flows in very strong static stability. Recall that the flux Richardson number is defined as the ratio of the consumption of turbulent kinetic energy (TKE) caused by the negative buoyancy forces, $-\beta F_\theta$, to the shear generation of the TKE, $\tau dU/dz$:

$$\mathrm{Ri}_f = \frac{-\beta F_\theta}{\tau dU/dz}. \quad (8)$$

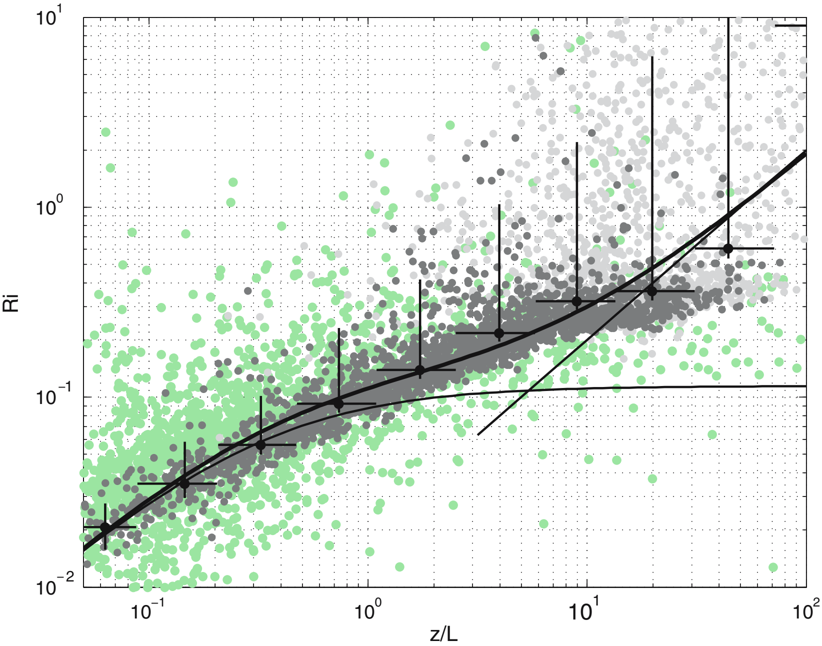

Fig. 3 Gradient Richardson number, Ri, within and above the ABL versus dimensionless height z/L, after the NS ABL data from LES DATABASE64 (dark grey points are for $z < h$ and light grey points, for $z > h$) and observational data from the field campaign SHEBA (green points). Heavy black points with error bars (one standard deviation above and below each point) show the bin-averaged values of Ri after the DATABASE64. The bold curve shows Eq. 10 with Φ_H taken after Eq. 11b, $C_{U1} = 2$, $C_{\Theta 1} = 1.6$ and $C_{\Theta 2} = 0.2$; the steep thin line shows its asymptote: Ri $\sim z/L$; and the thin curve with a plateau (unrealistic in the upper part of the ABL) shows Eq. 10 with the traditional, linear approximation of $\Phi_H = 1 + 2z/L$

Ri_f (in contrast to the gradient Richardson number, Ri) cannot grow infinitely, otherwise the TKE consumption would exceed its production. Hence Ri_f at very large ξ should tend to a limit, $\mathrm{Ri}_\mathrm{f}^\infty$ (= 0.2 according to currently available experimental data, see Zilitinkevich et al. 2007b). Then solving Eq. 8 for dU/dz and substituting $\mathrm{Ri}_\mathrm{f}^\infty$ for Ri_f gives the asymptote

$$\frac{dU}{dz} \to \frac{\tau^{1/2}}{\mathrm{Ri}_f^\infty L}, \tag{9}$$

which in turn gives $\Phi_M \to k(Ri_f^\infty)^{-1}\xi$, and thus rehabilitates Eq. 4 for Φ_M. The gradient Richardson number becomes

$$\mathrm{Ri} \equiv \frac{\beta d\Theta/dz}{(dU/dz)^2} = \left(\frac{k^2}{k_T}\right) \frac{\xi \Phi_H(\xi)}{(1 + C_{U1}\xi)^2}. \tag{10}$$

Therefore to ensure unlimited growth of Ri with increasing ξ (in other words, to guarantee "no critical Ri"), the asymptotic ξ dependence of Φ_H should be stronger than linear. Recalling that the function Φ_H at small ξ is known to be close to linear, a reasonable compromise could be a quadratic polynomial [recall the above quoted conclusion of Esau and Byrkjedal (2007) that $C_{\Theta 1}$ in Eq. 4b increases with increasing z/L).

On these grounds we adopt the approximations $\Phi_M = 1 + C_{U1}\xi$ and $\Phi_H = 1 + C_{\Theta 1}\xi + C_{\Theta 2}\xi^2$ covering both the TN and NS ABL. To extend them to the CN and LS ABL, we

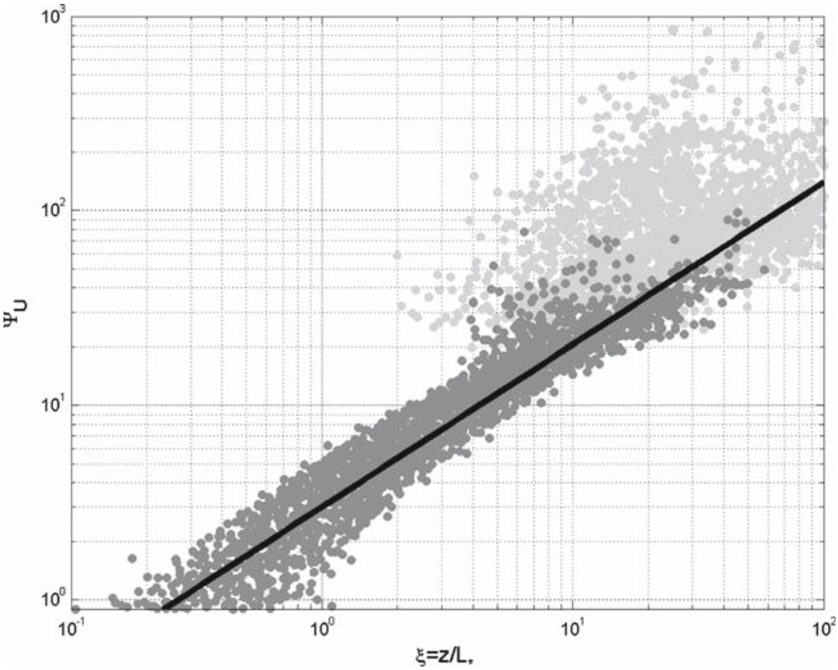

Fig. 4 The wind-speed characteristic function $\Psi_U = k\tau^{-1/2}U - \ln(z/z_{0u})$ versus dimensionless height $\xi = z/L_*$, after the LES DATABASE64. Dark grey points show data for $z < h$; light grey points, for $z > h$. The line shows Eq. 13a with $C_U = 3.0$

employ the generalised scaling, Eqs. 6–7:

$$\Phi_M = 1 + C_{U1}\frac{z}{L_*}, \tag{11a}$$

$$\Phi_H = 1 + C_{\Theta 1}\frac{z}{L_*}\xi + C_{\Theta 2}\left(\frac{z}{L_*}\right)^2. \tag{11b}$$

Comparing Eqs. 9 and 11a gives $\mathrm{Ri}_f^\infty = kC_{U1}^{-1}$. Then taking conventional values of $\mathrm{Ri}_f^\infty = 0.2$ and $k = 0.4$ gives an *a priori* estimate of C_{U1}= 2.

Figures 1 and 2 show Φ_M and Φ_H vs. $\xi = z/L_*$ after the LES DATABASE64 (Beare et al. 2006; Esau and Zilitinkevich, 2006), which includes the TN, CN, NS, and LS ABLs. Figure 2 confirms that the ξ dependence of Φ_H is indeed essentially stronger than linear: With increasing ξ, the best-fit linear dependence $\Phi_H = 1+2\xi$ shown by the thin line diverge from data more and more, and at $\xi \gg 1$ becomes unacceptable. The steeper thin line shows the quadratic asymptote $\Phi_H = 0.2\xi^2$ relevant only for very large ξ. Figure 1 confirms the expected linear dependence. Both figures demonstrate a reasonably good performance of Eq. 11 over the entire ABL depth (data for $z < h$ are indicated by dark grey points) and allows determining the constants $C_{U1} = 2$ (coinciding with the above *a priori* estimate), $C_{\Theta 1} = 1.6$ and $C_{\Theta 2} = 0.2$, with the traditional values of the von Karman constants: $k = 0.4$ and $k_T = 0.47$. For comparison, data for $z > h$ (indicated by light grey points) quite expectedly exhibit wide spread. The composite scale L_* is calculated after Eqs. 6–7 with $C_N = 0.1$ and $C_f = 1$.

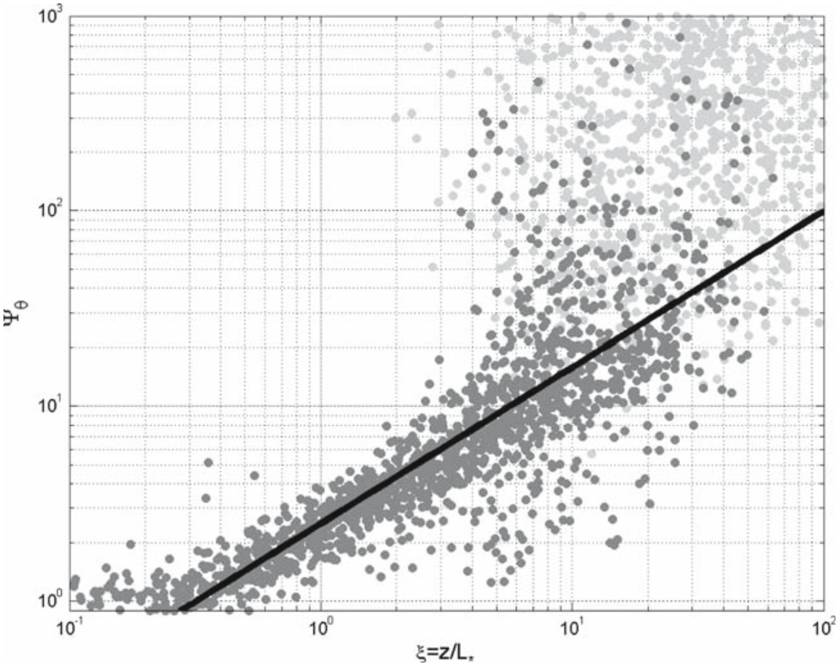

Fig. 5 Same as in Fig. 4 but for the potential-temperature characteristic function $\Psi_\Theta = k_T \tau^{-1/2} (\Theta - \Theta_0) (-F_\theta)^{-1} - \ln(z/z_{0u})$. The line shows Eq. 13b with $C_\Theta = 2.5$

Figure 3 shows the gradient Richardson number, Eq. 10, vs. z/L after the LES data for the TN and NS ABL (indicated by dark and light grey points, as in Figs. 1 and 2) and data from meteorological mast measurements at about 5, 9 and 13 m above the snow surface in the field campaign SHEBA (Uttal et al. 2002) indicated by green points. The bold curve shows our approximation of $\mathrm{Ri} = k^2 k_T^{-1} \xi \Phi_H \Phi_M^{-2}$—taking Φ_M and Φ_H after Eq. 11 with $C_{U1} = 2$, $C_{\Theta 1} = 1.6$ and $C_{\Theta 2} = 0.2$; the thin curve shows the traditional approximation of Ri—taking Φ_M and Φ_H after Eq. 4 with $C_{U1} = 2$ and $C_{\Theta 1} = 2$ (it affords a critical value of Ri≈0.17); and the steep thin line shows the asymptotic behaviour of our approximation, $\mathrm{Ri} \sim z/L$, at large z/L. Heavy points with error bars are the bin-averaged values after LES DATABASE64.

This figure demonstrates consistency between the LES and the field data for such a sensitive parameter as Ri (the ratio of gradients—inevitably determined with pronounced errors). For our analysis this result is critically important. It allows using the LES DATABASE64 on equal grounds with experimental data. Recall that in using LES we have the advantage of fully controlled conditions, which is practically unachievable in field experiments.

We give here one example: dealing with LES data we are able to distinguish between data for the ABL interior, $z < h$ (indicated in our figures by dark grey points) and data for $z > h$ (indicated by light grey points). As seen in Fig. 3, the gradient Richardson number within the ABL practically never exceeds 0.25–0.3, although turbulence is observed at much larger Ri. This observation perfectly correlates with the recent theoretical conclusion that Ri ~ 0.25 is not the critical Ri in the traditional sense (the border between turbulent and laminar regimes) but a threshold separating the two turbulent regimes of essentially different nature: strong, fully developed turbulence at Ri $\ll 0.25$; and weak, intermittent turbulence at Ri $\gg 0.25$

(Zilitinkevich et al. 2007b). These two are just the regimes typical of the ABL and the free atmosphere, respectively.

3 Surface fluxes

The above analysis clarifies our understanding of the physical nature of the stable ABL but does not immediately give flux–profile relationships suitable for practical applications. To receive analytical approximations of the mean wind and temperature profiles, $U(z)$ and $\Theta(z)$, across the ABL, we apply the generalised similarity theory presented in Sect. 2 to "characteristic functions":

$$\Psi_U = \frac{kU(z)}{\tau^{1/2}} - \ln\frac{z}{z_{0u}}, \tag{12a}$$

$$\Psi_\Theta = \frac{k_T\tau^{1/2}\left[\Theta(z) - \Theta_0\right]}{-F_\theta} - \ln\frac{z}{z_{0u}}, \tag{12b}$$

and employ LES DATABASE64 to determine their dependences on $\xi = z/L_*$.

Results from this analysis presented in Figs. 4 and 5 are quite constructive. Over the entire ABL depth, Ψ_U and Ψ_Θ show practically universal dependences on ξ that can be reasonably accurately approximated by the power laws:

$$\Psi_U = C_U\xi^{5/6}, \tag{13a}$$

$$\Psi_\Theta = C_\Theta\xi^{4/5}, \tag{13b}$$

with C_U= 3.0 and C_Θ= 2.5.

The wind and temperature profiles become

$$\frac{kU}{\tau^{1/2}} = \ln\frac{z}{z_{0u}} + C_U\left(\frac{z}{L}\right)^{5/6}\left[1 + \frac{(C_N N)^2 + (C_f f)^2}{\tau}L^2\right]^{5/12}, \tag{14a}$$

$$\frac{k_T\tau^{1/2}(\Theta - \Theta_0)}{-F_\theta} = \ln\frac{z}{z_{0u}} + C_\Theta\left(\frac{z}{L}\right)^{4/5}\left[1 + \frac{(C_N N)^2 + (C_f f)^2}{\tau}L^2\right]^{2/5}, \tag{14b}$$

where $C_N = 0.1$ and $C_f = 1$ (see discussion of Eq. 7). Given $U(z)$, $\Theta(z)$ and N, Eqs. 14a, b allow determination of the turbulent fluxes, τ and F_θ, and the Obukhov length, $L = \tau^{3/2}(-\beta F_\theta)^{-1}$, at the computational level z. Numerical solution to this system is simplified by the fact that the major terms on the right-hand sides are the logarithmic terms, and moreover, the second terms in square brackets are usually small compared to unity. Hence iteration methods should work efficiently. As a first approximation N, unknown until we determine the ABL height, is taken $N = 0$. In the next iterations, it is calculated using Eq. 18.

Given τ and F_θ, the surface fluxes are calculated using dependencies:

$$\frac{\tau}{\tau_*} = \exp\left[-3\left(\frac{z}{h}\right)^2\right], \tag{15a}$$

$$\frac{F_\theta}{F_*} = \exp\left[-2\left(\frac{z}{h}\right)^2\right]. \tag{15b}$$

For details see Zilitinkevich and Esau (2005) and Esau and Byrkjedal (2007).

The ABL height, h, required in Eq. 15 is calculated using the multi-limit h model (Zilitinkevich et al. 2007a, and references therein) consistent with the present analysis. The diagnostic version of this model determines the equilibrium ABL height, h_E:

$$\frac{1}{h_E^2} = \frac{f^2}{C_R^2 \tau_*} + \frac{N|f|}{C_{CN}^2 \tau_*} + \frac{|f \beta F_*|}{C_{NS}^2 \tau_*^2}, \tag{16}$$

where C_R= 0.6, C_{CN}= 1.36 and C_{NS}= 0.51 are empirical dimensionless constants.

More accurately h can be calculated using the prognostic, relaxation equation (Zilitinkevich and Baklanov 2002):

$$\frac{\partial h}{\partial t} + \vec{U} \cdot \nabla h - w_h = K_h \nabla^2 h - C_t \frac{u_*}{h_E}(h - h_E), \tag{17}$$

which therefore should be incorporated in a numerical model employing our scheme. In Eq. 17, h_E is taken after Eq. 16, w_h is the mean vertical velocity at the height $z = h$ (available in numerical models), the combination $C_t u_* h_E^{-1}$ is the inverse ABL relaxation time scale, $C_t \approx 1$ is an empirical dimensionless constant, and K_h is the horizontal turbulent diffusivity (the same as in other prognostic equations of the model under consideration).

Finally, given h, the free-flow Brunt-Väisälä frequency, N, is determined through the root-mean-square value of the potential temperature gradient over the layer $h < z < 2h$:

$$N^4 = \frac{1}{h} \int_h^{2h} \left(\beta \frac{\partial \Theta}{\partial z} \right)^2 dz \tag{18}$$

and substituted into Eq. 14 for the next iteration.

Some problems (first of all, air–sea interaction) require not only the absolute value of the surface momentum flux, $\vec{\tau}_*$, but also its direction. Recalling that our method allows determination of the ABL height, h, and therefore the wind vector at this height, $\vec{U}_h$, the problem reduces to the determination of the angle, α_* between $\vec{U}_h$ and $\vec{\tau}_*$. For this purpose we employ the cross-isobaric angle formulation:

$$\sin \alpha_* = \frac{-fh}{kU_h} \left[-2 + 10 \frac{(-\beta F_* h)^2}{\tau_*^3} + 0.225 \frac{(Nh)^2}{\tau_*} + 10 \frac{(fh)^2}{\tau_*} \right], \tag{19}$$

based on the same generalised similarity theory as the present paper (see Eqs. 7b, 41b, 43 and Fig. 4 in Zilitinkevich and Esau (2005)).

Following the above procedure, Eqs. 14–18 allow calculating the following parameters:

- turbulent fluxes τ(z) and F_θ(z) at any computational level z within the ABL,
- surface fluxes, $\vec{\tau}_*$ and F_*,
- ABL height, h,[either diagnostically after Eq. 16 or more accurately, accounting for its evolution after Eqs. 16–17].

Empirical constants that appear in the above formulations are given in Table 1.

The proposed method can be applied, in particular, to the shallow ABL, when the lowest computational level is close to h, and standard approaches completely fail. But it has advantages also in situations when the ABL (the height interval $0 < z < h$) contains several computational levels. In such cases, it provides several independent estimates of h, u_*^2 and F_*, and by this means makes available a kind of data assimilation, namely, more reliable determination of h, u_*^2 and F_* through averaging over all estimates.

Table 1

Constant	In Equation	Comments
$k = 0.4,\ k_T = 0.47$	(1), (3), etc	traditional values
$C_N = 0.1,\ C_f = 1$	(7)	after Zilitinkevich and Esau (2005), slightly corrected
$C_{U1} = 2.0,\ C_{\Theta 1} = 1.6,\ C_{\Theta 2} = 0.2$	(11a,b)	after present paper; $C_{U1} = 2.0$ and $C_{\Theta 1} = 1.6$ correspond to the coefficients $\beta_1 = C_{U1}/k = 5.0$ and $\beta_2 = C_{\Theta 1}/k = 4.0$ in the log-linear laws formulated for $L = u_*^3(-k\beta F_*)^{-1}$
$C_U = 3.0,\ C_\Theta = 2.5$	(13), (14)	after present paper
$C_R = 0.6,\ C_{CN} = 1.36,\ C_{NS} = 0.51$	(16)	after Zilitinkevich et al. (2007a)
$C_t = 1$	(17)	after Zilitinkevich and Baklanov (2002)

4 Concluding remarks

In this paper we employ a generalised similarity theory for the stably stratified sheared flows accounting for non-local features of the atmospheric stable ABL, follow modern views on the turbulent energy transformations rejecting the critical Richardson number concept, and use recent, high quality experimental and LES data to develop analytical formulations for the wind speed and potential temperature profiles across the entire ABL.

Results from our analysis are validated using LES data from DATABASE64 covering the four types of ABL: truly neutral, conventionally neutral, nocturnal stable and long-lived stable. These LES are in turn validated through (shown to be consistent with) observational data from the field campaign SHEBA.

Employing generalised formulae for the dimensionless velocity and potential temperature gradients, Φ_M and Φ_H, Eq. 3, based on the composite turbulent length scale L_*, Eq. 7, and z-dependent turbulent velocity and temperature scales, $\tau^{1/2}$ and $F_\theta \tau^{-1/2}$, we demonstrate that Φ_M and Φ_H are to a reasonable accuracy approximated by universal functions of z/L_* (Φ_M linear, Φ_H stronger than linear) across the entire ABL.

Using the quadratic polynomial approximation for Φ_H, we demonstrate that our formulation leads to the unlimitedly increasing z/L dependence of the gradient Richardson number, Ri, consistent with both LES and field data and arguing against the critical Ri concept.

We employ the above generalised format to the deviations, Ψ_U and Ψ_Θ, Eq. 12, of the dimensionless mean wind and potential temperature profiles from their logarithmic parts [$\sim \ln(z/z_{0u})$] to obtain power-law approximations: $\Psi_U \sim (z/L_*)^{5/6}$ and $\Psi_\Theta \sim (z/L_*)^{4/5}$ that perform quite well across the entire ABL.

On this basis, employing also our prior ABL height model and resistance laws, we propose a new method for calculating the turbulent fluxes at the surface in numerical models.

Acknowledgements This work has been supported by the EU Marie Curie Chair Project MEXC-CT-2003-509742, ARO Project W911NF-05-1-0055, EU Project FUMAPEX EVK4-2001-00281, EU Project TEMPUS 26005, Norwegian Project MACESIZ 155945/700, joint Norway-USA Project ROLARC 151456/720, and NORDPLUS Neighbour 2006-2007 Project 177039/V11.

References

Ayotte KW, Sullivan PP, Andren A, Doney SC, Holtslag AAM, Large WG, McWilliams JC, Moeng C-H, Otte M, Tribbia JJ, Wyngaard J (1996) An evaluation of neutral and convective planetary boundary-layer parameterizations relative to large eddy simulations. Boundary-Layer Meteorol 79:131–175

Beare RJ, MacVean MK, Holtslag AAM, Cuxart J, Esau I, Golaz JC, Jimenez MA, Khairoudinov M, Kosovic B, Lewellen D, Lund TS, Lundquist JK, McCabe A, Moene AF, Noh Y, Raasch S, Sullivan P (2006) An intercomparison of large eddy simulations of the stable boundary layer. Boundary Layer Meteorol 118:247–272

Esau I, Byrkjedal Ø (2007) Application of large eddy simulation database to optimization of first order closures for neutral and stably stratified boundary layers. This issue of Boundary Layer Meteorol

Esau IN, Zilitinkevich SS (2006) Universal dependences between turbulent and mean flow parameters in stably and neutrally stratified planetary boundary layers. Nonlin Processes Geophys 13:135–144

Högström U (1996) Review of some basic characteristics of the atmospheric surface layer. Boundary-Layer Meteorol 78:215–246

Lenschow DH, Li XS, Zhu CJ, Stankov BB (1988) The stably stratified boundary layer over the Great Plains. Part 1: Mean and turbulence structure. Boundary-layer Meteorol 42:95–121

Monin AS, Obukhov AM (1954) Main characteristics of the turbulent mixing in the atmospheric surface layer. Trudy Geophys Inst AN SSSR 24(151):153–187

Nieuwstadt FTM (1984) The turbulent structure of the stable, nocturnal boundary layer. J Atmos Sci 41:2202–2216

Sorbjan Z (1988) Structure of the stably-stratified boundary layer during the SESAME-1979 experiment. Boundary-Layer Meteorol 44:255–266

Tjernstrom M, Zagar M, Svensson G, Cassano JJ, Pfeifer S, Rinke A, Wyser A, Dethloff K, Jones C, Semmler T, Shaw M (2004) Modelling the arctic boundary layer: an evaluation of six ARCMIP regional-scale models using data from the SHEBA project. Boundary-Layer Meteorol 117:337–381

Uttal T, 26 co-authors (2002) Surface heat budget of the arctic Ocean. Bull Amer Meteorol Soc 83:255–275

Wittich KP (1991) The nocturnal boundary layer over Northern Germany: an observational study. Boundary-Layer Meteorol 55:47–66

Yague C, Viana S, Maqueda G, Redondo JM (2006) Influence of stability on the flux-profile relationships for wind speed, phi-m, and temperature, phi-h, for the stable atmospheric boundary layer. Nonlin Processes Geophys 13:185–203

Zilitinkevich SS, Baklanov A (2002) Calculation of the height of stable boundary layers in practical applications. Boundary-Layer Meteorol 105:389–409

Zilitinkevich SS, Esau IN (2002) On integral measures of the neutral, barotropic planetary boundary layers. Boundary-Layer Meteorol 104:371–379

Zilitinkevich SS, Esau IN (2003) The effect of baroclinicity on the depth of neutral and stable planetary boundary layers. Quart J Roy Meteorol Soc 129:3339–3356

Zilitinkevich SS, Esau I (2005) Resistance and heat transfer laws for stable and neutral planetary boundary layers: old theory, advanced and ee-evaluated. Quart J Roy Meteorol Soc 131:1863–1892

Zilitinkevich SS, Grachev AA, Fairall CW (2001) Scaling reasoning and field data on the sea-surface roughness lengths for scalars. J Atmos Sci 58:320–325

Zilitinkevich SS, Perov VL, King JC (2002) near-surface turbulent fluxes in stable stratification: calculation techniques for use in general circulation models. Quart J Roy Meteorol Soc 128:1571–1587

Zilitinkevich SS, Esau I, Baklanov A (2007a) Further comments on the equilibrium height of neutral and stable planetary boundary layers. Quart J Roy Meteorol Soc (In press)

Zilitinkevich SS, Elperin T, Kleeorin N, Rogachevskii I (2007b) A minimal turbulence closure model for stably stratified flows: energy and flux budgets revisited. Submitted to this issue of Boundary Layer Meteorol